Phase Only Full Waveform Inversion of Elastic Data Using Acoustic Engine

Stuart Farris, Ettore Biondi, and Guillaume Barnier

ABSTRACT

Modeling the elastic earth with acoustic assumptions leads to large amplitude mismatches between observed and predicted data. Matching both amplitude and phase information between elastic field data and acoustic modeled data is more difficult than only matching phase information. Therefore, we attempt to perform acoustic full waveform inversion (FWI) with an objective function designed to favor minimizing phase variation between observed and predicted data.

INTRODUCTION

Seismic experiments observe wavefields that are propagated through an elastic earth. We try to create a model of the earth that predicts the elastic data we observe in the field. Full waveform inversion (FWI) provides an iterative technique to find such an earth model by matching observed field data to predicted model data (Tarantola, 1984). FWI has been shown to produce earth models with much higher resolution than competing methods (Sirgue et al., 2009). However, the high cost of FWI limits the complexity of its modeling capabilities. Therefore, FWI performed on large commercial datasets often models with acoustic wave propagation which is computationally cheaper than modeling with elastic propagation.

It should seem obvious that an inversion scheme that matches simplified, acoustic data with complex, elastic data will create incorrect models of the earth (Warner et al., 2012). Previous attempts have been made to rectify the differences between acoustic and elastic modeling. Namely, correcting acoustic propagation amplitudes by simulating elastic effects (Ben Veitch et al., 2012), using match filters to remove elastic effects from the initial observed data (Agudo et al., 2016), and conditioning the FWI objective function to minimize phase variations (Shen, 2014). The later approach will be applied here.

The method proposed by Shen (2014) uses an acoustic FWI engine, but performs an amplitude normalization within the objective function. This normalization steers the objective function to better match phase variations between the observed elastic and predicted acoustic data. The goal is to ignore the amplitude variations that cannot be matched because of the inherent differences between the two modeling techniques. In this report we evaluate the effectiveness of this technique by comparing its FWI results with those of standard acoustic FWI and elastic FWI.

THEORY

We redefine the objective function proposed by Shen (2014) in a more verbose manner:

$$\Phi(\mathbf{m}) = \frac{1}{2}\sum_{l=1}^{N_{traces}} \left|\left| \frac{\mathbf{d}_l^p}{||\mathbf{d}_l^p||} - \frac{\mathbf{d}_l^o}{||\mathbf{d}_l^o||} \right|\right|_2^2 = \frac{1}{2}\sum_{l=1}^{N_{traces}} \left|\left|\mathbf{r}_l^d\right|\right|_2^2 \tag{1}$$

where $\mathbf{m} \in \mathbb{R}^M$ defines our model space. $\mathbf{d}_l^p, \mathbf{d}_l^o \in \mathbb{R}^N$ are predicted traces and observed traces, respectively. $||\mathbf{d}_l||$ is the normalization term for a given trace, l, defined as:

$$||\mathbf{d}_l|| = \left(\sum_{t=1}^{N} d_{l,t}^2\right)^{\frac{1}{2}} \tag{2}$$

The residual $\mathbf{r}_l^d \in \mathbb{R}^N$ is the difference between one normalized predicted trace and one normalized observed trace. A physical interpretation of the objective function can be obtained by expanding Equation 1:

$$\Phi(\mathbf{m}) = \frac{1}{2}\left(\frac{\mathbf{d}_l^p}{||\mathbf{d}_l^p||} - \frac{\mathbf{d}_l^o}{||\mathbf{d}_l^o||}\right)^T \left(\frac{\mathbf{d}_l^p}{||\mathbf{d}_l^p||} - \frac{\mathbf{d}_l^o}{||\mathbf{d}_l^o||}\right) \tag{3}$$

$$= 1 - \frac{1}{2}\left(\frac{\mathbf{d}_l^p}{||\mathbf{d}_l^p||} \cdot \frac{\mathbf{d}_l^o}{||\mathbf{d}_l^o||}\right) \tag{4}$$

Minimizing the objective function can be interpreted as maximizing the zero lag cross correlation between the normalized predicted traces and normalized observed traces where the normalization term is the energy of each trace. The normalization weights the relative amplitudes of each trace so that maximizing the cross correlation corresponds to minimizing the phase difference between respective traces. This would be a true phase only inversion if we compared individual frequencies of individual arrival events. Here we find the limitation of this objective function since, of course, this is unfeasible in real applications. However, narrow band passes during this scheme's application make the comparison of multiple arrivals possible and move this objective function towards true phase only inversion (Shen, 2014).

To determine model update directions we need the derivative of the objective function. For simplicity we will consider a single trace:

$$\nabla_m \Phi(\mathbf{m}) = \frac{1}{2}\nabla_m ||\mathbf{r}^d||_2^2 \tag{5}$$

$$= \left(\frac{\partial \mathbf{r}^d}{\partial \mathbf{m}}\right)^T \mathbf{r}^d \tag{6}$$

$$= \left(\frac{\partial \mathbf{d}^p}{\partial \mathbf{m}}\right)^T \left(\frac{\mathbf{r}^d}{||\mathbf{d}^p||} - \frac{(\mathbf{r}^d)^T\mathbf{d}^p}{||\mathbf{d}^p||^3}\mathbf{d}^p\right) \tag{7}$$

$$= \mathrm{B}^T\tilde{\mathbf{r}}^d \tag{8}$$

We find that the derivative of the objective function is the adjoint of the Born operator applied to some normalized residual. The full derivation of the gradient can be found in the appendix. With the new objective function, Equation 1, and its derivative, Equation 7, we can perform a nonlinear conjugate gradient inversion scheme for our model $\mathbf{m}$.

OBSERVED DATA

To test the effectiveness of our inversion scheme, we conduct a seismic experiment in an elastic, synthetic model and invert for the pressure wave velocity. The elastic model is five kilometers wide, three kilometers deep, and includes a 500 meter water column. Figure 1 illustrates the pressure wave velocity, v_p, shear wave velocity, v_s, and density, ρ, of the model. The v_s/v_p ratio was chosen to be a constant, reasonable value of 1.75. The structure was created using a synthetic model generation code written by Clapp (2014). Using the true elastic model, seismic data is recorded at the surface with 50 shots spaced at 100 meters. Receivers are placed every 10 meters and record vertical and horizontal displacement.

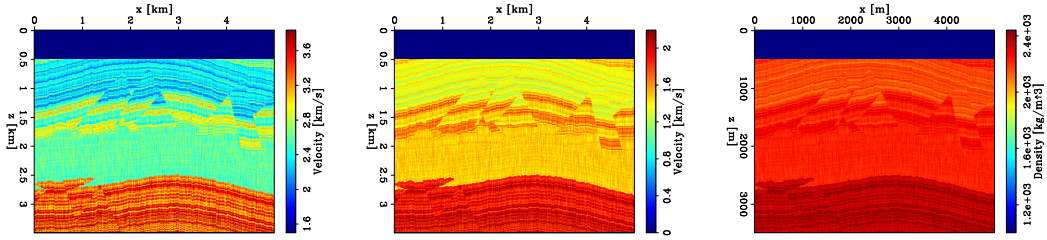

Figure 1: Elastic properties of synthetic model. Left: pressure wave velocity. Center: shear wave velocity. Right: density. [**CR**]

Figure 2 illustrates a sample shot gather with collected horizontal displacement, vertical displacement, and calculated pressure data. Pressure measurements can be calculated using,

$$P = \frac{1}{2}(\sigma_{xx} + \sigma_{zz}) \tag{9}$$

where σ_{xx} and σ_{zz} are the horizontal and vertical stress, respectively.

INVERSION PLAN

To evaluate the feasibility of the phase only acoustic FWI, we will compare our v_p model results with elastic FWI results and basic acoustic FWI results. Each FWI application was solved using the nonlinear solver created by Ettore Biondi and Guillaume Barnier (Biondi and Barnier, 2017).

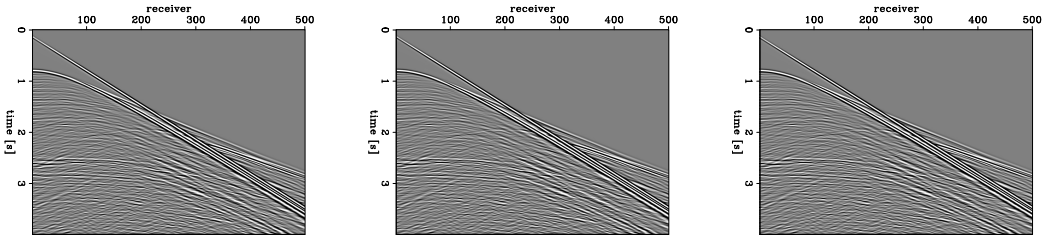

Figure 2: Example shot gather from elastic pressure data. Left: σ_{xx} Center: σ_{zz}. Right: Pressure. [**CR**]

When we perform elastic propagation to produce pressure data, we inject a source term with components in the x and z directions. But, when inverting with our acoustic phase only engine we need to inject the an equivalent acoustic source wavelet that only has one component. Using a least squares regression we can invert for the acoustic wavelet that corresponds to the elastic wavelet used to create the observed data. The original elastic wavelet, a Ricker wavelet with a dominant frequency of 20 Hz, and the inverted acoustic wavelet are illustrated in Figure 3.

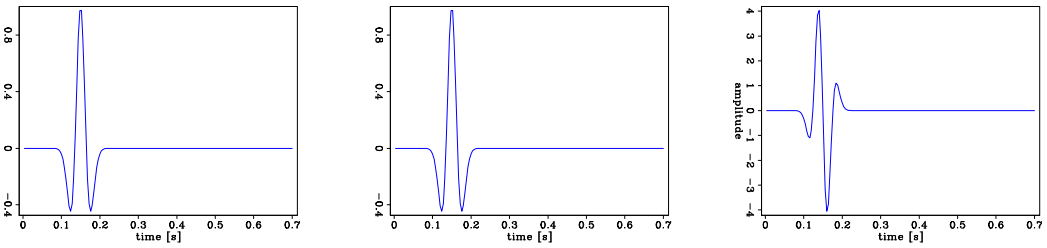

Figure 3: Left: x component of elastic source term. Center: z component of elastic source term. Right: inverted acoustic source. [**CR**]

The starting model for the FWI applications is a smoothed version of Figure 1. Bunks et al. (1995) showed an upscaling inversion is better at avoiding local minimum. Following this method, we will begin Each FWI scheme with a bandpass of 5 Hz and perform 40 conjugate gradient iterations. The result of this 5 Hz inversion will be the starting model for the next inversion which uses a 10 Hz bandpass. This scaling proceeds up to 25 Hz.

This is the framework we will use to compare our phase only acoustic FWI to traditional elastic and acoustic FWI.

ACKNOWLEDGMENTS

This investigation would be significantly delayed if not for all those who contributed to the nonlinear solver in Biondi and Barnier (2017). We would also like to thank Robert Clapp for creating the elastic model used in this report. We thank the affiliates of the Stanford Exploration Project for their continued support.

REFERENCES

Agudo, O. C., N. da Silva, M. Warner, and J. Morgan, 2016, Acoustic full-waveform inversion in an elastic world, *in* SEG Technical Program Expanded Abstracts 2016, 1058–1062, Society of Exploration Geophysicists.

Ben Veitch, James Rickett, and James Hobro, 2012, Imaging elastic media by corrections to acoustic propagation: Presented at the .

Biondi, E. and G. Barnier, 2017, A flexible out-of-core solver for linear/non-linear problems: SEP-Report, **168**.

Bunks, C., F. M. Saleck, S. Zaleski, and G. Chavent, 1995, Multiscale seismic waveform inversion: Geophysics, **60**, 1457–1473.

Clapp, R., 2014, Synthetic model building using a simplied basin modeling approach: SEP-Report, **155**, 143–150.

Shen, X., 2014, Early-arrival waveform inversion for near-surface velocity estimation: PhD thesis.

Sirgue, L., O. I. Barkved, J. P. Van Gestel, O. J. Askim, and J. H. Kommedal, 2009, 3d waveform inversion on Valhall wide-azimuth OBC: Presented at the 71st EAGE Conference and Exhibition incorporating SPE EUROPEC 2009.

Tarantola, A., 1984, Inversion of seismic reflection data in the acoustic approximation: Geophysics, **49**, 1259–1266.

Warner, M., J. Morgan, A. Umpleby, I. Stekl, and L. Guasch, 2012, Which physics for full-wavefield seismic inversion?: Presented at the 74th EAGE Conference and Exhibition incorporating EUROPEC 2012.